

Article

A Novel Wideband Transition from LTCC Laminated Waveguide to Air-Filled Rectangular Waveguide for W-band Applications

Bin Yuan ^{1,2}, Qing Du ³, Chengxiang Hao ¹, Yan Zhao ¹ and Zhongjun Yu ^{1,2,*}¹ Aerospace Information Research Institute, Chinese Academy of Sciences, Beijing 100190, China² School of Electronic, Electrical and Communication Engineering, University of Chinese Academy of Sciences, Beijing 100190, China³ School of Information and Communication Engineering, Communication University of China, Beijing 100024, China

* Correspondence: yuzj@ucas.ac.cn

Abstract: In this paper, a novel wideband transition from a laminated waveguide (LWG) to an air-filled rectangular waveguide (RWG) is proposed for millimeter-wave integration solutions based on multilayer low-temperature co-fired ceramic (LTCC) technology. The integrated transition cavity is divided into several resonators by introducing five grounded via holes. Due to the magnetic wall existing in the symmetry plane, the equivalent circuit of the proposed transition can be simplified as a three-pole filter model to explain the working mechanism with wideband performance. A W-band integrated LWG-to-RWG transition is designed as an example using LTCC technology. Two back-to-back prototypes with different lengths are fabricated and measured. A measured 25.7% bandwidth from 76 GHz to 101 GHz can be achieved for return loss better than 14 dB. The average insertion loss of a single transition is about 0.5 dB. The compact structure and wideband performance give it potential in high-density millimeter-wave and terahertz packaging.

Keywords: air-filled rectangular waveguide; laminated waveguide; low-temperature co-fired ceramic (LTCC); transition; W-band; wideband



Citation: Yuan, B.; Du, Q.; Hao, C.; Zhao, Y.; Yu, Z. A Novel Wideband Transition from LTCC Laminated Waveguide to Air-Filled Rectangular Waveguide for W-band Applications. *Micromachines* **2023**, *14*, 52. <https://doi.org/10.3390/mi14010052>

Academic Editors: Alina-Cristina Bunea, Martino Aldrigo and Dan Neculoiu

Received: 12 December 2022

Revised: 20 December 2022

Accepted: 24 December 2022

Published: 25 December 2022



Copyright: © 2022 by the authors. Licensee MDPI, Basel, Switzerland. This article is an open access article distributed under the terms and conditions of the Creative Commons Attribution (CC BY) license (<https://creativecommons.org/licenses/by/4.0/>).

1. Introduction

With the gradual depletion of spectrum resources, the high-frequency bands of millimeter-wave (MMW) and even the terahertz (THz) band become increasing attractive in large-bandwidth wireless systems such as high-resolution radars and high-speed wireless communications [1]. The precision processing technology of print circuits is necessary to achieve advanced MMW/THz integrated modules and systems. An integrated solution based on a thin-film circuit process is a good choice for the THz band due to its low-loss and stable performance [2], but the single-layer scheme limits the design flexibility and circuit density. Low-temperature co-fired ceramic (LTCC) technology can highly integrate multiple devices in multilayer dielectric substrate, which meets the design requirements of high precision and miniaturization of MMW/THz electronic products [3]. Compact laminated waveguide (LWG) based on LTCC technology has been widely used to solve the problems of radiation loss of microstrip transmission lines in the high MMW band, which is suitable for MMW/THz integration and packaging. However, the signal interface of the MMW/THz packaging module is generally formed with an air-filled rectangular waveguide (RWG) due to the superior features of excellent durability and low insertion loss [4]. Therefore, the integrated transition between LWG and air-filled RWG is crucial for MMW/THz LTCC packaging modules.

In the past decades, various approaches have been presented to achieve the transition from a substrate-integrated waveguide to an air-filled RWG based on traditional printed

circuit board (PCB) technology [5–9]. However, the permittivity of LTCC dielectric substrate is high. It is quite a challenge to obtain wideband performance with the transition from LWG to air-filled RWG due to the dimension mismatch and huge impedance difference between them. Several earlier works of LWG-to-RWG transitions based on LTCC technology have been reported [10–13]. The integrated LTCC prototype of LWG-to-RWG transition is first presented in [10] and gives an effective bandwidth of over 8% in Ka-band. To miniaturize the transition structure, a compact configuration is designed to take advantage of the limited volume in substrate near the air-filled RWG aperture [11]. In [12], an extra air cavity is introduced in the LTCC laminated substrate to improve impedance matching, expanding the simulated bandwidth to 10.8% with a compromise of fabrication complexity.

In this paper, a novel LWG-to-RWG transition with large bandwidth and compact size is proposed for W-band LTCC applications. To obtain wideband performance, five grounded via holes are strategically arranged in the transition cavity to generate a simplified three-pole filter model, which produces three reflection zeros in the passband. The integrated LTCC transition is fabricated and measured. Measured results are in good agreement with simulated ones.

2. Transition Design and Analysis

2.1. Configuration and Working Mechanism

Figure 1 gives the multilayer configuration of the proposed LTCC transition from the LWG to the air-filled RWG. The LTCC laminated waveguide consists of four dielectric layers and five metal layers and is directly mounted on the vertical RWG port. The aperture size of the bottom metal layer M5 is the same as the cross-section of a standard air-filled RWG. An enclosed three-layer (M2–M5) transition cavity above the RWG port is surrounded by a metalized via-hole fence to prevent energy leakage. The whole transition structure is designed to occupy as minimal a space as possible around the RWG port.

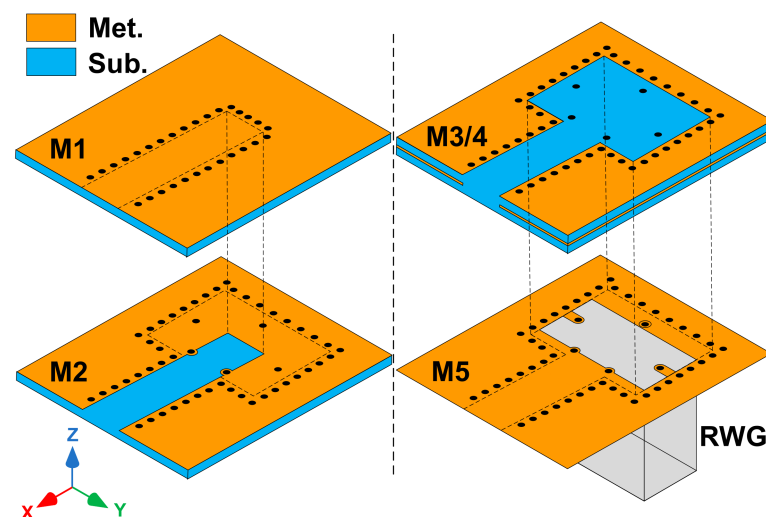


Figure 1. Exploded view of proposed transition with four layers of LTCC dielectric substrate.

As shown in Figure 2a, the LWG in the first layer is inserted above the transition cavity. The insertion length LS is about half the waveguide wavelength to create an equivalent resonator, marked as ‘1’. It can be seen from Figure 2b that five grounded via holes divide the three-layer transition cavity into four half-wavelength resonators marked as ‘2’, ‘3’, ‘4’, and ‘5’, respectively. The region and position of each equivalent resonator are denoted with dotted circles in Figure 2. Obviously, the whole transition is a symmetric structure, and there is a virtual magnetic wall (VMW) at the symmetry plane. Therefore, the resonators on both sides of the magnetic wall are isolated from each other, and no coupling power crosses the magnetic wall, which simplifies the equivalent filter model of the proposed transition. As illustrated in Figure 3, a three-pole filter model with an LWG source and an RWG load is

created by three Resonators 1, 2, and 3, which can be used to predict the performance of the transition. The input LWG is coupled with Resonator 2 by a coefficient M_{S2} . The coupling coefficients M_{12} , M_{13} , M_{23} represent the mutual coupling between the three resonators. Resonators 2 and 3 are coupled with the output air-filled RWG by coupling coefficients M_{L2} and M_{L3} , respectively. According to the proposed filter topology and cross-coupled theory, there will be three reflection zeros in the passband, and two prescribed transmission zeros can be generated with an appropriate coupling matrix.

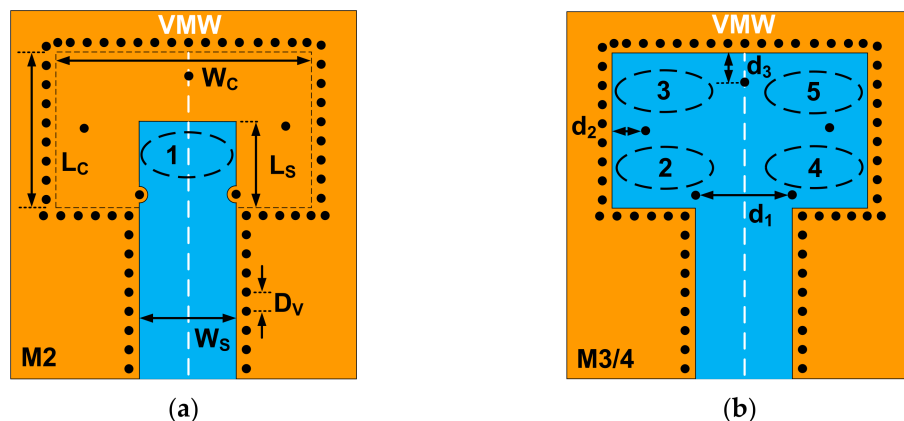


Figure 2. Top view of the proposed transition: (a) top metal layer M2; (b) middle metal layer M3 and M4.

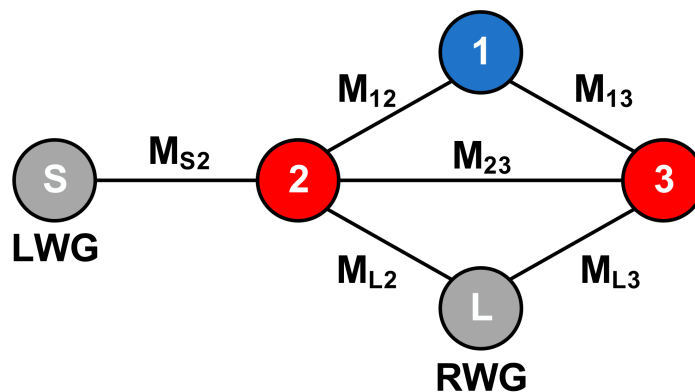


Figure 3. Equivalent filter model of the proposed transition.

2.2. Design and Simulation

In order to validate the feasibility of the proposed transition scheme and the equivalent model, a W-band design is investigated. The height of the single-layer LTCC substrate is taken as 0.096 mm, and the thickness of the gold metal layer is 0.008 mm. Ferro A6M with permittivity of 5.9 and loss tangent of 0.002 is chosen as the dielectric material of the LTCC substrate. The standard rectangular waveguide WR10 of 2.54 mm × 1.27 mm is used in this design. Full-wave electromagnetic simulation is executed with the physical structure shown in Figure 1. The dimensions of the transition cavity L_c and W_c are crucial to the eigen frequency of Resonators 2 and 3, while the insertion length L_s influences the eigen frequency of Resonator 1. The distance d_1 between two via holes on the entrance of the transition cavity determines the coupling from the LWG port to Resonator 2. The distance d_2 is a key parameter for the coupling between Resonator 2 and Resonator 3. In addition, a via hole with distance d_3 from the cavity edge is arranged on the VMW plane to adjust the impedance matching.

The three-pole filter model presented in Figure 3 is employed to explain and guide the transition design. The desired transmission response can be obtained by an appropriate coupling matrix using the classical filter synthesis method [14]. The center fre-

quency and bandwidth are set as 88.5 GHz and 25 GHz, respectively. The coupling coefficients are specified as follows: $M_{S2} = 1.3374$, $M_{11} = -0.3313$, $M_{12} = 0.3934$, $M_{13} = 1.2432$, $M_{22} = -0.1532$, $M_{23} = 0.1953$, $M_{33} = 0.4023$, $M_{L2} = -1.0939$, and $M_{L3} = 0.7694$. Additionally, two transmission zeros are caused by the cross-couplings of M_{L2} and M_{23} . The S-parameter results of the equivalent model and full-wave simulation are demonstrated in Figure 4. The key parameters mentioned above are optimized to achieve the expected transition response. Table 1 gives the detailed dimensions of the optimized transition. As shown in Figure 4, the full-wave simulation result exhibits wideband performance, and it is in good agreement with the synthesis result of the equivalent three-pole filter model. The return loss of a single transition is better than 20 dB from 76 GHz to 101 GHz (28.2% bandwidth). Moreover, the E-field distribution with a different phase is shown in Figure 5. It is obvious that Resonator 2 and Resonator 4 are first excited by the input LWG, and they are coupled with Resonator 1. Then, the energy flows pass through Resonator 1 and couple to Resonator 3 and Resonator 5. This coupling path is the mainline coupling, and there are still other cross couplings in the transition. It can be demonstrated that the equivalent three-pole filter model is effective for the proposed transition scheme.

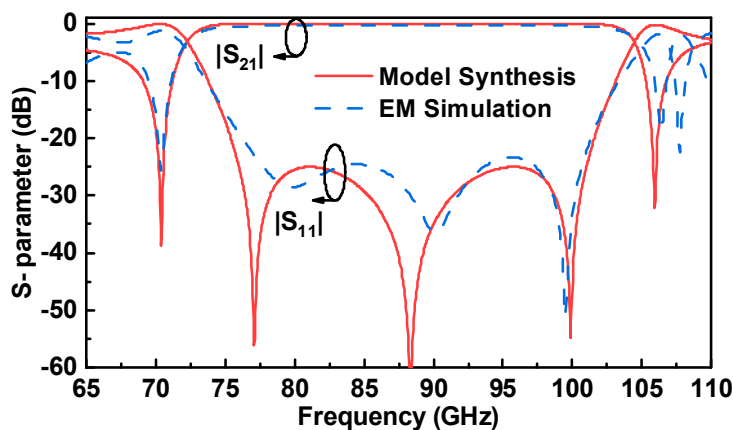


Figure 4. S-parameters comparison between classical filter synthesis and full-wave electromagnetic simulation of the proposed single transition.

Table 1. Dimension parameters of the proposed transition (unit: mm).

L_C	W_C	L_S	W_S	D_V	d_1	d_2	d_3
1.75	2.54	0.86	0.92	0.18	0.85	0.25	0.23

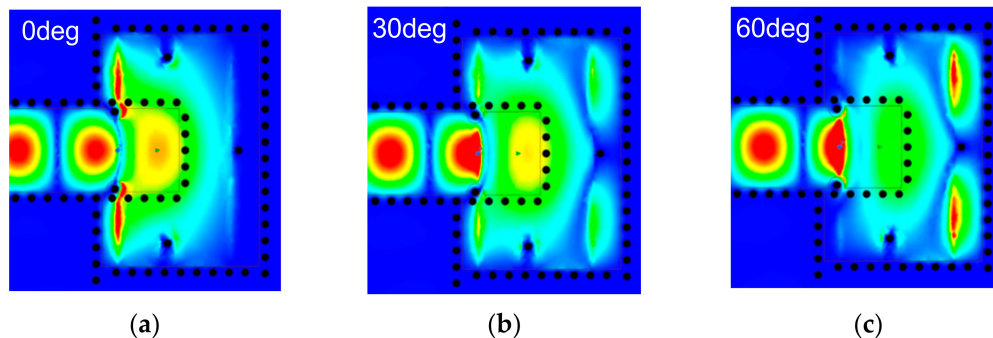
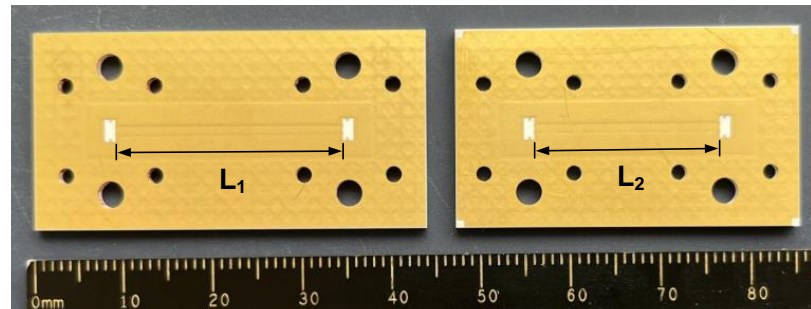


Figure 5. E-field distribution in the proposed transition with different phases: (a) Phase = 0°; (b) Phase = 30°; and (c) Phase = 60°.

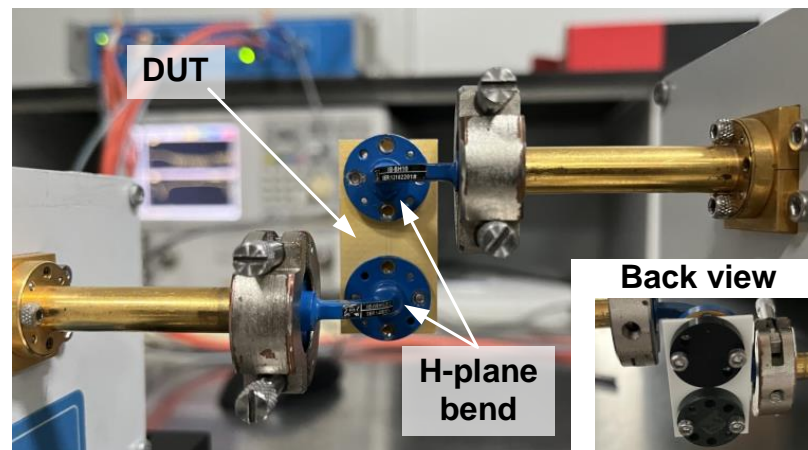
3. Fabrication and Measurement

To characterize the transmission performance of the single transition with different interfaces, two back-to-back prototypes with different lengths are fabricated and measured.

Figure 6a is a photograph of two fabricated LTCC modules, in which the LWG lengths are, respectively, set to $L_1 = 25$ mm and $L_2 = 20$ mm. The back-to-back module is tested using a network analyzer combined with two W-band frequency extenders, and it is assembled with two H-plane 90° waveguide bends to facilitate measurement, as shown in Figure 6b. Four screws are used to tightly fix the LTCC module to the waveguide bends. The washers help to distribute the pressure to avoid cracking the LTCC substrate during measurement.



(a)



(b)

Figure 6. (a) Photograph of the fabricated back-to-back transitions. (b) Measurement setup.

The simulated and measured results of two back-to-back transitions are given in Figure 7. From the different measured insertion loss of two transitions, the transmission loss of the LTCC laminated waveguide can be estimated. The insertion loss of the back-to-back transition can be calibrated by subtracting the transmission loss of the LWG line, half of which is the insertion loss of the single transition. The measured results demonstrate that the return loss is better than 14 dB in the range from 78 GHz to 101 GHz (25.7% bandwidth). The measured insertion loss of two back-to-back transitions with different length are, separately, 3 dB and 2.6 dB on average, and the transmission loss of the 10 mm LWG is calculated as about 0.8 dB. Therefore, it can be derived that the calibrated insertion loss of a single transition is about 0.5 dB in the operating band. The slight discrepancy between the simulation and the measured results may be due to the fabrication tolerance, assembly errors, and leakage wave caused by the waveguide gap. Compared with the previous LTCC works listed in Table 2, the proposed transition in this paper exhibits great bandwidth and low-loss performance without compromising structure size.

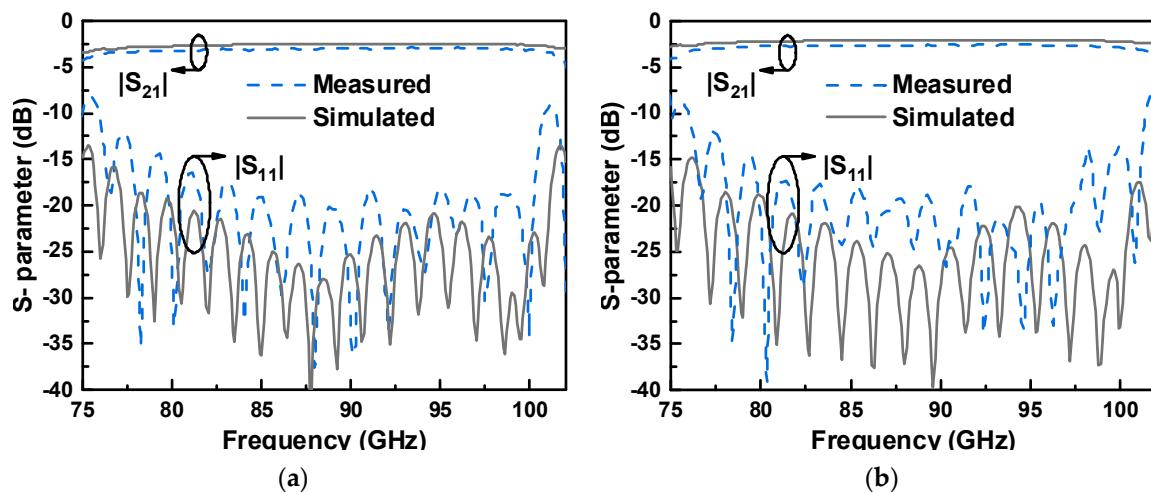


Figure 7. Simulated and measured results of two back-to-back transitions with an (a) LWG length of L_1 and (b) an LWG length of L_2 .

Table 2. Comparison with previous LTCC LWG-to-RWG transitions.

Reference	Frequency (GHz)	Insertion Loss (dB)	Return Loss (dB)	Fractional Bandwidth	Footprint (λ_c^2)
[10]	27.8–30.3	0.4	15	8.6%	0.73×0.69
[11]	34.8–37.8	0.26	13	8.3%	0.53×1.03
[12]	76–81	1.05	10	6.4%	0.29×0.41
This work	78–101	0.5	14	25.7%	0.52×0.75

4. Conclusions

A novel compact LWG-to-RWG transition with large bandwidth is presented for W-band LTCC integrations. Five grounded via holes are introduced to separate the transition cavity into several resonators. The working principle is interpreted by an equivalent three-pole filter model that is demonstrated to be effective for the proposed transition. The back-to-back prototypes are fabricated and measured with good performance. The compact size and wide bandwidth make the proposed transition applicable in LTCC integrated systems.

Author Contributions: Conceptualization, B.Y. and Q.D.; methodology, B.Y., Q.D. and Z.Y.; software, B.Y., Q.D. and C.H.; validation, B.Y. and Y.Z.; formal analysis, B.Y., Q.D. and C.H.; investigation, B.Y. and Z.Y.; resources, Z.Y., Y.Z. and C.H.; writing—original draft preparation, B.Y.; writing—review and editing, Q.D., C.H. and Z.Y.; visualization, B.Y. and Q.D.; supervision, C.H., Y.Z. and Z.Y.; project administration, Z.Y.; funding acquisition, C.H., Y.Z. and Z.Y. All authors have read and agreed to the published version of the manuscript.

Funding: This work was supported by the Foundations of Chinese Academy of Sciences under grants E0Z221010F and E0H3210203.

Data Availability Statement: Not applicable.

Conflicts of Interest: The authors declare no conflict of interest.

References

- Mittleman, D.M. Perspective: Terahertz science and technology. *J. Appl. Phys.* **2017**, *122*, 230901. [[CrossRef](#)]
- Yuan, B.; Wu, P.; Yu, Z.; Hao, C. Wideband End-Wall Transition From Microstrip to Waveguide With via-Less Choke Structure for Terahertz Application. *IEEE Trans. Terahertz Sci. Technol.* **2022**, *12*, 317–320. [[CrossRef](#)]
- Lee, J.-H.; DeJean, G.; Sarkar, S.; Pintel, S.; Lim, K.; Papapolymerou, J.; Laskar, J.; Tentzeris, M.M. Highly integrated millimeter-wave passive components using 3-D LTCC system-on-package (SOP) technology. *IEEE Trans. Microw. Theory Tech.* **2005**, *53*, 2220–2229. [[CrossRef](#)]

4. Song, H.-J. Packages for Terahertz Electronics. *Proc. IEEE* **2017**, *105*, 1121–1138. [[CrossRef](#)]
5. Mohamed, I.; Sebak, A. Broadband Transition of Substrate-Integrated Waveguide-to-Air-Filled Rectangular Waveguide. *IEEE Microw. Wirel. Compon. Lett.* **2018**, *28*, 966–968. [[CrossRef](#)]
6. Liu, K.; Wu, P.; Zhang, J. Wideband RWG-SIW Interconnection With Improved Integration for Millimeter-Wave/Terahertz Application. *IEEE Microw. Wirel. Compon. Lett.* **2022**, *32*, 835–838. [[CrossRef](#)]
7. Glogowski, R.; Zurcher, J.-F.; Peixeiro, C.; Mosig, J.R. Broadband Ka-band rectangular waveguide to substrate integrated waveguide transition. *Electron. Lett.* **2013**, *49*, 602–604. [[CrossRef](#)]
8. Zhu, K.; Xiao, Y.; Tan, W.; Luo, H.; Sun, H. A Broadband E-Band Single-Layer-SIW-to-Waveguide Transition for Automotive Radar. *IEEE Microw. Wirel. Compon. Lett.* **2022**, *32*, 523–526. [[CrossRef](#)]
9. Hassan, E.; Scheiner, B.; Michler, F.; Berggren, M.; Wadbro, E.; Röhrli, F.; Zorn, S. Multilayer Topology Optimization of Wideband SIW-to-Waveguide Transitions. *IEEE Trans. Microw. Theory Techn.* **2020**, *68*, 1326–1339. [[CrossRef](#)]
10. Huang, Y.; Wu, K.L. A broadband LTCC integrated transition of laminated waveguide to air-filled waveguide for millimeter wave applications. *IEEE Trans. Microw. Theory Tech.* **2003**, *51*, 1613–1617. [[CrossRef](#)]
11. Huang, X.B.; Wu, K.L. A Ka-band broadband integrated transition of air-filled waveguide to laminated waveguide. *IEEE Microw. Wirel. Compon. Lett.* **2012**, *22*, 515–517. [[CrossRef](#)]
12. Lee, J.G.; Hirokawa, J.; Ando, M. Transition to a high-dielectric constant post wall waveguide from a standard waveguide by using a hollow cavity in a laminated substrate. In Proceedings of the 2006 IEEE Antennas and Propagation Society International Symposium, Albuquerque, NM, USA, 9–14 July 2006. [[CrossRef](#)]
13. Wang, X.; Stelzer, A. A 79-GHz LTCC laminated waveguide to metallic rectangular waveguide transition using high permittivity material. In Proceedings of the 40th European Microwave Conference, Paris, France, 28–30 September 2010. [[CrossRef](#)]
14. Cameron, R.J. General coupling matrix synthesis methods for Chebyshev filtering functions. *IEEE Trans. Microw. Theory Tech.* **1999**, *47*, 433–442. [[CrossRef](#)]

Disclaimer/Publisher’s Note: The statements, opinions and data contained in all publications are solely those of the individual author(s) and contributor(s) and not of MDPI and/or the editor(s). MDPI and/or the editor(s) disclaim responsibility for any injury to people or property resulting from any ideas, methods, instructions or products referred to in the content.